The long-range organization of a native photosynthetic membrane

Raoul N. Frese*†‡, C. Alistair Siebert§, Robert A. Niederman¶, C. Neil Hunter§, Cees Otto†, and Rienk van Grondelle*

*Biophysics, Faculty of Sciences, Vrije Universiteit Amsterdam, De Boelelaan 1081, Amsterdam 1081 HV, The Netherlands; †Biophysical Techniques Group, Department of Science and Technology, University of Twente, P.O. Box 217, 7500 AE Enschede, The Netherlands; §Department of Molecular Biology and Biotechnology, University of Sheffield, Sheffield S10 2TN, United Kingdom; and ¶Department of Molecular Biology and Biochemistry, Rutgers, The State University of New Jersey, Piscataway, NJ 08854

Edited by Pierre A. Joliot, Institut de Biologie Physico-Chemique, Paris, France, and approved November 17, 2004 (received for review October 1, 2004)

Photosynthesis relies on the delicate interplay between a specific set of membrane-bound pigment–protein complexes that harvest and transport solar energy, execute charge separation, and conserve the energy. We have investigated the organization of the light-harvesting (LH) and reaction-center (RC) complexes in native bacterial photosynthetic membranes of the purple bacterium *Rhodobacter sphaeroides* by using polarized light spectroscopy, linear dichroism (LD) on oriented membranes. These LD measurements show that in native membranes, which contain LH2 as the major energy absorber, the RC–LH1–PufX complexes are highly organized in a way similar to that which we found previously for a mutant lacking LH2. The relative contribution of LH1 and LH2 light-harvesting complexes to the LD spectrum shows that LH2 preferentially resides in highly curved parts of the membrane. Combining the spectroscopic data with our recent atomic force microscopy (AFM) results, we propose an organization for this photosynthetic membrane that features domains containing linear arrays of RC–LH1–PufX complexes interspersed with LH2 complexes and some LH2 found in separate domains. The study described here allows the simultaneous assessment of both global and local structural information on the organization of intact, untreated membranes.

membrane organization | photosynthesis | polarized spectroscopy

Photosynthetic purple bacteria are among the oldest species known (1, 2). Within the class of photosynthetic organisms, they have specialized in growing on low-energy photons under dim light conditions (3). The main characteristic of the photosystems of these bacteria is their "less is more" design: They are constructed by the repetitive use of identical protein units as building blocks, resulting in highly symmetric pigment–protein complexes ("rings") with carefully tuned light-absorption properties. Protein-bound chromophores, carotenoids and bacteriochlorophylls (BChls), are the light-interacting functional groups that carry out the photosynthetic process: the conversion of light energy into a stable charge separation. The incoming light is collected by specialized light-harvesting (LH) complexes, and, by means of intra- and intercomplex energy transfer, the excitation energy is transported to a reaction center (RC). Here charge separation takes place, which fuels subsequent electron- and proton-transfer reactions that build up the transmembrane electrochemical gradient that is eventually used for the formation of ATP.

Photosynthetic purple bacteria may contain two different types of pigment–protein complexes involved in energy- and electron-transfer reactions: the RC–LH1 core complexes and the peripheral light-harvesting complex 2 (LH2). Both LH complexes are composed of two concentric rings of roughly circularly arranged α-helices that bind the carotenoid and BChl pigments. The peripheral LH2 feeds its excitations into LH1, which surrounds the RC, enabling efficient energy transfer from the LH1 BChls to the primary RC energy acceptor/electron donor: a special pair of strongly coupled BChls (P) (4). The RC consists of two branches of electron-transfer cofactors arranged around a C_2 symmetry axis. In addition to the special pair, each branch contains another "monomeric" BChl and a bacteriopheophytin (BPheo) molecule. Light-driven charge separation occurs along the so-called active (or L branch) of pigments, where the electron within a few picoseconds is transferred via the monomeric BChl to the BPheo. In the case of the purple bacterium, *Rhodobacter sphaeroides*, the encirclement of the RC by the LH1 helices is perturbed by a small, α-helical polypeptide, PufX, which is proposed to function as a passage for the quinols, which are photoreduced by the RC (5, 6). Furthermore, it is well established that PufX induces the dimerization of the RC–LH1 core complexes *in vivo* (7, 8). The peripheral LH2 complex is not a prerequisite for photosynthesis but can be synthesized by the bacterium in varying amounts to increase the absorption cross section for harvesting sunlight. Three-dimensional structures are available for all of the individual components: the LH2 complex, the core RC–LH1–PufX complex (9, 10), and the subsequent energy-transducing components, the cytochrome bc_1 complex and the ATP-synthase complex (11, 12).

As a whole, the photosynthetic pigment–proteins interact functionally within a multicomplex network, which is localized in a specialized membrane. Given their individual structures, the organization of the complexes within the membrane can be visualized by various techniques. Information on individual membrane patches can be derived from atomic force microscopy (AFM) topographs (13–15). In the special case of a membrane exhibiting close to crystallographic order, electron microscopy (EM) has been applied successfully (7, 8). Nevertheless, these techniques do not suffice to address the overall organization of proteins within an entire, intact membrane. Moreover, these techniques require treatment and preparation methods that partially perturb the membrane structure.

Polarized spectroscopy on oriented membranes has proven to be a nonperturbative tool with which to investigate membrane organization (16). A linear-dichroism (LD) experiment probes the difference in absorption between horizontally and vertically polarized light by oriented complexes, and, thus, the orientation of the transition-dipole moments of the chromophores relative to the orientation axis of the complex can be obtained (17, 18). Similarly, one can probe oriented membranes or membrane fragments, but an LD signal will be measured only if there is some macroscopic order in the system. Such measurements performed on membranes of *Rb. sphaeroides* that lacked the peripheral LH2 complex, both in the presence of and without PufX, demonstrated the occurrence of a special orientation of the RC within the LH1 ring, but only when PufX was present. This "PufX effect" could be detected only because of the long-range ordering of the protein complexes within the photosynthetic membrane. The structural basis of the long-range

This paper was submitted directly (Track II) to the PNAS office.

Abbreviations: LH, light-harvesting; RC, reaction center; LD, linear dichroism; AFM, atomic force microscopy; BChl, bacteriochlorophyll; BPheo, bacteriopheophytin; P, primary electron donor; Q, quinone; LH1 and LH2, light-harvesting complex 1 and 2.

‡To whom correspondence should be addressed. E-mail: raoul@nat.vu.nl.

www.pnas.org/cgi/doi/10.1073/pnas.0407295102

ordering in LH2$^-$–PufX$^+$ membranes was provided by a negative-stain EM investigation on similar membranes, which showed that RC–LH1–PufX complexes are arranged as dimers (7). The structural basis of the PufX effect has recently been provided by a negative-stain EM study of membranes with and without PufX (8). This work on LH2$^-$ membranes showed that, in the absence of PufX, the RC–LH1 complexes can no longer form tubular membranes consisting of dimers, which results in a completely altered membrane morphology with flattened sheets containing monomeric complexes.

Here we report the results of LD spectroscopy to investigate the orientation of the RC within the LH1 ring in membranes that do contain LH2; these are oriented, intact native membranes isolated from photosynthetically grown *Rb. sphaeroides*. Our data show a remarkable resemblance between the LD and light-minus-dark LD-difference signals of native membranes and those reported before on the LH2$^-$ deletion strain (19). We conclude that, as observed for LH2$^-$–PufX$^+$ membranes (7, 8, 19), native membranes possess an ordered, long-range supraorganization of the RC–LH1–PufX core complexes that appears to be an intrinsic property of this species. A comparison between the signals of intact chromatophores and patches prepared from the same chromatophores indicates an abundance of LH2 complexes in highly curved domains. Combining the results from this study with the recently obtained AFM images on patches of the same membranes studied here (13), we have modeled the arrangement of the photosynthetic complexes within the native *Rb. sphaeroides* membrane.

Materials and Methods

Biological Membranes. Cells of *Rb. sphaeroides* NCIB 8253 were grown photosynthetically at moderate light intensity (500 W·m^{-2}) for 18–20 h, followed by a switch to high light intensity (825 W·m^{-2}) for 4 h. Intracytoplasmic membrane vesicles (chromatophores) were isolated by rate-zonal sucrose density-gradient centrifugation (20). These chromatophores are intact photosynthetic membranes, and the same preparations that were used in the AFM studies (13) were used for this study. For the primary LD experiments, we probed intact, untreated chromatophores. These vesicles were opened up and converted into patches of membrane by using a small amount of detergent (0.03% β-dodecyl maltoside), as for the AFM study (13), to investigate the effect of the curvature of intact chromatophores on the spectroscopy.

Sample Preparation. Membranes were diluted with 10 mM Tris·HCl, pH 8.0. For low-temperature measurements, glycerol was added at a concentration of 70% (vol/vol). For the LD measurements, the sample was mixed with 14.5% (wt/vol) acrylamide and 0.5% *N*,*N*′-methylenebisacrylamide, and polymerized into a polyacrylamide gel by the addition of 0.05% ammonium persulfate and 0.03% *N*,*N*,*N*′,*N*′-tetramethylethylenediamine (TEMED, Sigma). Subsequently, the gel was compressed in two perpendicular directions (*x* and *y* axes), allowing it to expand along the *z* axis. The samples were cooled to 77 K in an Oxford liquid-nitrogen cryostat. The whole process of polymerizing, compressing, and freezing was performed in the dark.

Spectroscopy. Absorption (*A*), P$^+$ − P ΔA, LD, and P$^+$ − P ΔLD spectra were recorded on a home-built spectrapolarimeter with a resolution of 1.5 nm. P$^+$ − P ΔLD spectra were obtained by laser excitation at 670 nm to avoid photoselection by the polarized light [Coherent CR599 CW dye laser, with DCM dye (1 nm bandwidth), pumped by a Coherent Innova 310 argon ion laser]. The laser power was attenuated to 10 mW·cm^{-2} to achieve maximum signal. Absorbance and LD spectra were simultaneously measured by using two parallel lock-in amplifiers, one for the transmission (*A*) signal and the other for the vertical–horizontal difference absorption (LD) signal by using a monochromator with 1-nm resolution. The ΔLD spectra were directly recorded by using a third lock-in amplifier with the LD signal as input and locked to a 20-Hz laser modulation. For the ΔLD experiment, the LD signal was measured with a short (3-ms) integration time. This configuration allows the simultaneous measurements of absorbance, LD, and ΔLD spectra. The P$^+$ − P ΔA measurement was performed with two lock-in amplifiers in series with the laser at the same excitation wavelength as before, modulated with a chopper at a slow (20-Hz) frequency (16). To obtain the "unpolarized" ΔA spectrum, the transmission signal was modulated by using two perpendicularly placed polarizers with a PhotoElasticModulator (PEM 80, Hinds, Hillsboro, OR), which changes the polarization of the probing light from parallel to perpendicular, with 20 kHz, placed in between.

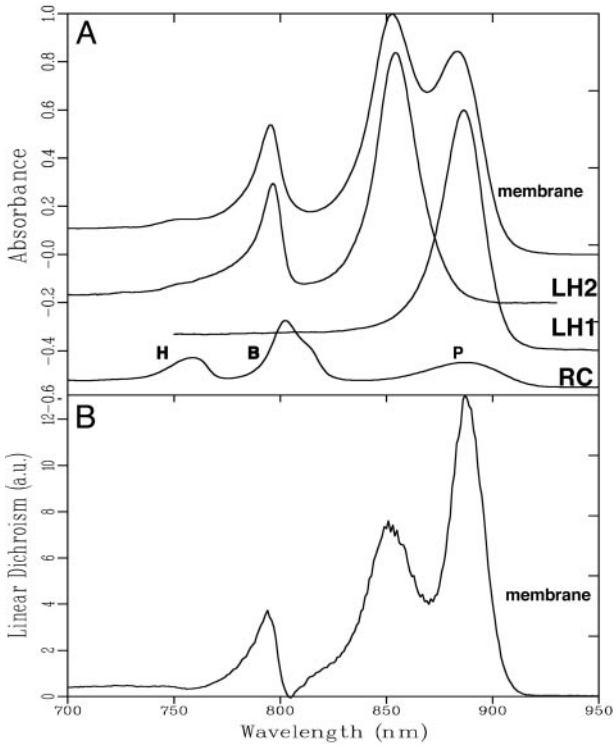

Fig. 1. Absorbance and LD spectra of intact photosynthetic membranes of *Rb. sphaeroides*. (*A*) The near-IR absorption spectra of native membranes and LH1-only, LH2-only, and RC-only membranes at 77 K. In the RC spectrum, P indicates the special pair, B the accessory BChls, and H the BPheos. The absorption of the RC complexes has been enhanced ×3 for ease of comparison. (*B*) The LD spectrum of native membranes at 77 K in the same spectral region. The LD spectra of LH1 and LH2 are similar to their absorption spectra. a.u., arbitrary units.

Results and Discussion

Whole, intact, and untreated membranes were diluted and oriented in a polyacrylamide gel as described in *Materials and Methods*. To reduce the spectral congestion all measurements have been performed at 77 K.

Absorption. Fig. 1*A* shows the near-IR absorbance spectrum of the membranes together with the spectra of the individual components: RC, LH1, and LH2. The LH1 and LH2 spectra have been scaled according to their contribution to the membrane spectrum; the RC spectrum has been magnified ×3 for clarity. Clearly, the absorption bands of the LH complexes dominate the membrane spectrum. The LH1 absorption spectrum consists of a single, broad band with a maximum at 880 nm; the LH2 absorption spectrum exhibits two main bands, the B800 band around 795 nm and the B850 band

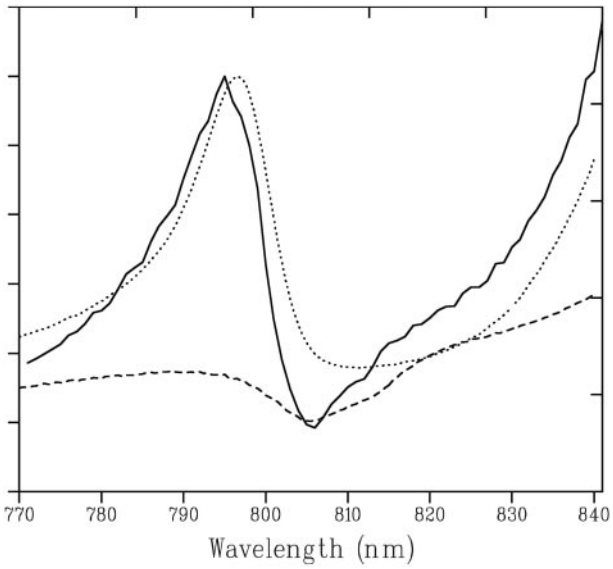

Fig. 2. Comparison between the 77 K LD spectra around 800 nm of native membranes (solid line), LH2 (dotted line), and $LH2^{-}$–$PufX^{+}$ membranes (dashed line).

around 850 nm. These bands originate from 30 (LH1) and 18 (LH2, B850) strongly interacting BChls and 9 (LH2, B800) weakly interacting BChls, respectively (9, 10). The magnitude of the absorbance bands of LH2 at 850 nm and LH1 at 870 nm points toward a 2:1 ratio of LH2:LH1 complexes. The RC absorption spectrum arises from the pigments located on the two RC branches: the special pair, P, at 880 nm, two monomeric BChls, B_L and B_M, at 800–810 nm, and the two pheophytins at 750 nm. In the membrane spectrum, the absorption spectrum of the RC is almost completely hidden by the absorption of the LH complexes; only the BPheos (H) are visible.

LD. The LD spectrum of the membranes, which is shown in Fig. 1*B*, roughly resembles the membrane absorption spectrum. This reflects the fact that the transition dipole moments of the BChls of both LH complexes are oriented in a very similar way. The main difference with the OD spectrum lies in the magnitude of the LH2 LD signal, which is approximately half of that of the LH1 signal (when normalized to the OD). This implies a possible difference in organization or orientation within the membranes between LH2 and LH1 complexes because both LH complexes have a very similar orientation of their BChls, hence a similar magnitude of LD signal is expected (9, 10, 21). The origin of this difference was investigated further by probing the LD spectrum of fragments of chromatophores and will be discussed in a separate paragraph below.

The negative feature just above 750 nm can be assigned to the near-IR absorption spectra transitions of the two pheophytins in the RC, which are known to be oriented with an angle of about 70° relative to the plane of the membrane (18, 22). Close inspection of the membrane LD spectrum also reveals a negative contribution at 805 nm, which slightly reduces the positive signal of the LH2 B800 BChls. Fig. 2 shows a comparison of the LD of the native membranes both with the LD of membranes of a mutant lacking LH2, but possessing the full RC–LH1–PufX machinery (dashed line) and LH2-only complexes (dotted line). Clearly the LD spectra of both the native membranes and the LH2-lacking membranes exhibit a similar negative feature at 805 nm, which is not present in the LH2-only sample. This negative LD signal at 805 nm has been reported before for the $LH2^{-}$ mutant and was assigned to the accessory BChls in the RC (19). It was also reported that in RC-only strains and in RC–LH1 strains without PufX, the accessory BChls show a positive LD (19). It was shown that this reversal in sign of the LD signal of the accessory BChls can be explained only if the RC assumes a special, nonrandom, orientation within the LH1 ring and also if a large majority of all RC–LH1 core complexes are aligned in regular arrays. It was concluded that the presence of PufX is a prerequisite for this effect to occur (19). It is striking to see that the organizing effect of PufX, previously observed only in the mutant lacking LH2, also occurs in native membranes. This phenomenon implies that the same, or very similar, regular LH1–RC arrays are formed despite the possibly disturbing presence of LH2. This observation, therefore, rules out many of the previously proposed models, at least in *Rb. sphaeroides*, for the organization of the LHs and RCs in the bacterial membrane, which suggested that dimeric (23) or monomeric (21, 24) LH1–RC complexes are fully surrounded by LH2 complexes.

Although native membranes naturally contain PufX, the observation is surprising, given that the presence of LH2 might have disturbed the formation of core arrays or might have given rise to differently oriented arrays in different membranes. The observation is also unexpected because the nine B800 BChls of each individual LH2 complex could have obscured any effect of the RC orientation for the two accessory BChls also absorbing at 800 nm. Fortuitously, because of the relative decrease of the LD signal of the LH2 complexes compared with that of the LH1 complexes in the membrane (thus, also compared to that of the RC, which is attached to LH1), the RC orientation has become visible in the LD spectrum.

ΔLD. The orientation of the RC in the LH1 ring, as proposed for the $LH2^{-}$ membranes (19), implies that the 880-nm Q_y transitions of the special pair are oriented almost perpendicular with respect to the long axis of the membrane. To examine whether this orientation of the RC in the LH1 ring also holds true for membranes containing LH2, it is necessary to obtain the LD spectrum of P in native membranes. However, in the membrane LD spectrum, the signal of P cannot be observed because it is obscured by the overlapping signal of the 30 LH1 BChls. This situation can be resolved by recording a light-minus-dark LD-difference spectrum that records the change of the membrane LD upon photooxidation of P. This ΔLD technique is especially suitable for LH2-containing membranes because the LH2 complex adds two more absorption bands at 800 and 850 nm, now almost fully obscuring the RC transitions over the available spectral window. Fig. 3 shows the change in native membrane absorbance (ΔOD, *A*) and LD (ΔLD, *B*) induced by photooxidation of P (solid line). For comparison, the spectra of the strain lacking LH2 but including PufX ($LH2^{-}$–$PufX^{+}$) have been included (dashed line). The difference-absorption spectrum shows the disappearance of the absorption band of the special pair and the electrochromic bandshift signals of the other RC and LH1 pigments because of the formation of P^{+}. Strikingly, the ΔLD signal of native membranes resembles, to a large extent, that of the $LH2^{-}$–$PufX^{+}$ strain. As seen for the $LH2^{-}$–$PufX^{+}$ strain, the special pair in native membranes exhibits a negative LD signal (≈890 nm), which is not observed for RC-only or RC–LH1 membranes without PufX. Although the magnitude of the bandshift signals of the accessory BChl and BPheo pigments appears to be lower in native membranes compared with the LH2-lacking mutant, the signs of all of the transitions are identical for both membranes. We therefore conclude that the organization of the LH1–RC complexes in native membranes closely resembles the organization proposed for the $LH2^{-}$–$PufX^{+}$ mutant.

Patches of Native Chromatophores. To investigate the origin of the decrease in magnitude of LD of LH2 compared with LH1 and of ΔLD of the accessory BChls and BPheos of the RC in native

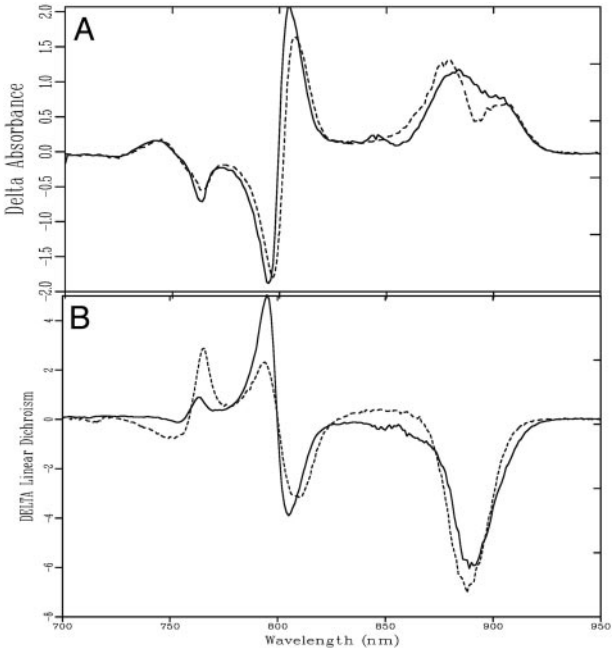

Fig. 3. Dark-minus-light absorption spectrum (*A*) and dark-minus-light LD spectrum (ΔLD) (*B*) of native membranes (solid line) and LH2$^-$–PufX$^+$ membranes (dashed line) at 77 K. Both spectra are normalized on OD.

chromatophores and LH2-lacking RC–LH1–PufX membranes, we probed the same preparation of opened-up membrane vesicles previously used for AFM imaging (13). Fig. 4 shows the absorbance and LD spectra (*A*) and ΔLD spectrum (*B*, upper spectrum) of patches of chromatophores. For comparison we included the ΔLD spectrum of the LH2$^-$–PufX$^-$ mutant reported before (19) (*B*, lower spectrum). In contrast to intact chromatophores (Fig. 1), no reduction in magnitude of the LD of LH2 relative to LH1 can be observed. Although the AFM images indicate a slight tilt of complexes within the membrane, such a small difference cannot explain the large reduction reported here. Another observation in that AFM study was the

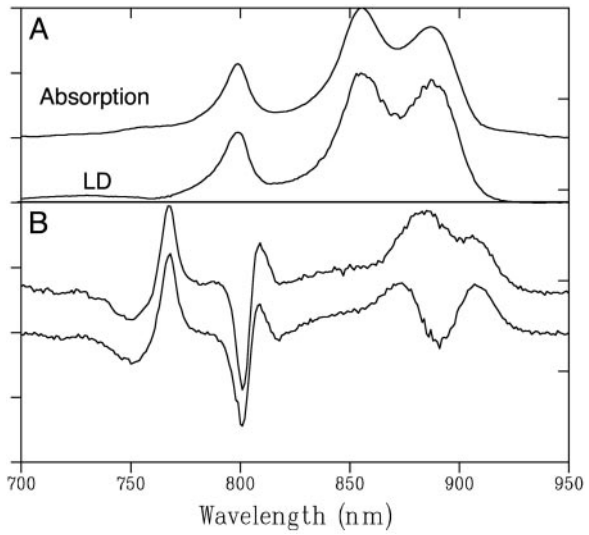

Fig. 4. The main near-IR absorption and LD spectra of fragmented native membranes (*A*) and dark-minus-light LD spectra (ΔLD) of fragmented native membranes (*B*, upper spectrum) and LH2$^-$–PufX$^-$ membranes (*B*, lower spectrum) at 77 K. Both spectra are normalized on OD.

abundance of LH2 complexes in membrane patches that were more curved than the areas of membrane where the majority of RC–LH1–PufX complexes were found. Likely, adhesion to the mica surface reduced the curvature of these particular membrane patches, which is more pronounced in intact chromatophores. An abundance of LH2 complexes in more curved regions explains a decrease in LD relative to LH1: the curvature will lead to an extra anisotropy for LH2 relative to LH1. The transition dipole moments of the B850 BChls are not oriented exactly perpendicular to the orientation axis (25), which causes a reduction of the averaged LD signal.

The ΔLD spectrum of the fragments is highly similar to that of the LH2 lacking PufX$^-$ mutant we reported previously (Fig. 4*B*) (19). These fragments do not show the ordering fingerprint of the special pair (a strong negative peak at 870 nm) but, instead, a positive signal is measured, superimposed on the LH1 bandshift. Also, the signs of the ΔLD signal of the accessory BChls are opposite to what we found for the intact chromatophores and the LH2$^-$–PufX$^+$ mutant. Despite the fact that the AFM shows individual membrane patches containing RC–LH1–PufX core complexes in linear arrays (13), compressing a gel containing an ensemble of such patches does not satisfy the prerequisites for measuring orientation effects in LD. It must be the case that the patches do not align similarly with respect to the orientation axis, and/or oriented patches contain arrays not similarly oriented with respect to the orientation axis, despite being individually composed of highly ordered RCs.

Strikingly, the magnitude of the bandshift signals of the accessory BChls and BPheos is the same for the fragments as for the PufX$^-$ mutant, whereas this is not the case for the intact chromatophores and the PufX$^+$ mutant. This situation is similar to the effect on the LD of LH2 (Fig. 1), and it is indicative of the remaining anisotropy on curved chromatophores compared with the isotropic situation for the tubular RC–LH1–PufX membranes lacking LH2. The LD signal of the special pair of the RC is not affected because the transition dipole is oriented almost perpendicular to the long axis of the membrane (19).

Model of the Membrane. The results presented in this study are supported by the recent AFM images on patches of the same photosynthetic membranes studied here (13) but flattened onto a mica surface, which show that RC–LH1–PufX complexes are arranged as linear rows of dimers interspersed with rows of LH2 complexes. The fact that the arrays generally do not appear exactly colinearly aligned is likely to be a consequence of opening up a spherical membrane, followed by adhesion of the membranes to the mica substrate. These procedures, which are unavoidable for high-resolution imaging, can disturb the native arrangement. Combining LD and AFM results, we can arrange the arrays in a regular fashion to produce the supraorganization of the photosynthetic membrane. Fig. 5 represents a model of a chromatophore from photosynthetically grown *Rb. sphaeroides*. The homogeneity in the size and shape of the membranes is verified by negative-stain EM, which shows semispherical membranes with a diameter of ≈80 nm (results not shown). More particularly, the preparation does not contain a significant amount of tubular membranes because such membranes were never observed in the AFM study (13). The various aspects of this model are as follows: (*i*) chromatophores are semispherical but contain a preferential long axis; (*ii*) the RCs have a unique orientation within the LH1 ring; (*iii*) RC–LH1–PufX complexes are arranged as rows of dimers interspersed with single or double rows of LH2 complexes; (*iv*) the rows are colinearly aligned; (*v*) these rows are drawn with a slight angle to the long axis to clarify the formation of a tubular membrane when LH2 is lacking (8, 19); (*vi*) the chromatophores are densely packed with complexes; and (*vii*) LH2 complexes are abundant in curved domains.

We emphasize that the measurements are conducted on bulk sample, which implies that any orientational effect of the RC can

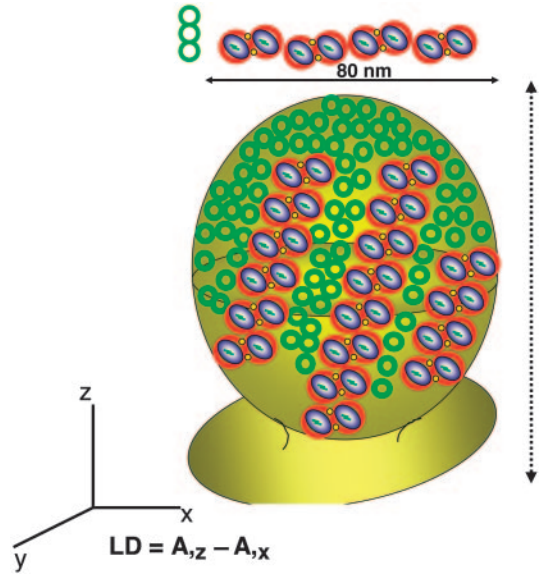

Fig. 5. A model for the organization of RC–LH1 core and LH2 complexes in a native, untreated membrane of *Rb. sphaeroides*. The geometry of our measurement is shown relative to the long axis of the chromatophore with LD defined as the absorption of vertically polarized light ($A_{,z}$) minus the absorption of horizontally polarized light ($A_{,x}$). A native intracytoplasmic membrane is depicted as an invagination of the membrane. The shape is a slightly distorted sphere to reflect an intrinsic asymmetry, tentatively drawn along the axis connecting the starting point of the invagination and the top (dashed vertical arrow depicts the long axis of orientation). RC–LH1 cores are shown as blue and white ovals enclosed by red circles and PufX, placed according to refs. 8, 10, and 19, is indicated in yellow. LH2 complexes are shown as green open circles. The near-IR absorption spectra transitions of the special pair of BChls (P) are represented by the bars within the blue and white ovals. Complexes and membrane are drawn to scale.

be seen only when a large majority of the RCs are oriented similarly in every single membrane. Moreover, the membranes should all display a similar orientation, otherwise the effect on the LD signal is lost. Although chromatophores are semispherical, for a preferential and general orientation to occur, some intrinsic and general asymmetry must exist. The point in the membrane where the invagination of the chromatophore starts could induce this asymmetry, resulting in an elongated membrane. Such a shape could also explain the difference in relative magnitude between the ΔLD signals of accessory BChls (B) and BPheos (H) in the native membranes as compared with the $LH2^-$ strain and the decrease in LD of the LH2 complexes in native membranes as compared with fragmented chromatophores. In contrast to the native membranes studied here, the $LH2^-$–$PufX^+$ membranes are known to be tubular. The regular arrays of core complexes along tubular membranes all contribute in a similar fashion to the LD and ΔLD spectrum. In contrast, regular arrays along an elongated, spherical shape show cancellation effects due to the out-of-plane components of the transition dipole moments in the highly curved top and bottom parts. These effects are much stronger for the B and, in particular, for the H pigments of the RC as compared with P because the special pair is oriented almost perpendicular to the long membrane axis. Similarly, a possible abundance of LH2 complexes in the curved parts of the membranes could account for their LD signal being smaller relative to that of LH1. A clustering of LH2 in such intracytoplasmic-membrane regions is suggested from membrane-biogenesis studies in which an increased curvature was observed in intracytoplasmic membrane with increasing LH2 levels (26).

The data presented here allow an estimate of the orientation of the RC within the LH1 ring. Indirectly, the ability to do so also demonstrates the structural integrity of the membrane: any movement of the complexes would disturb the high degree of organization of the RC complexes in the membrane as probed by the LD and ΔLD spectra.

The AFM images of some of the membrane fragments also showed an abundance of LH2 complexes, and these appeared difficult to image because of the relatively strong curvature of those particular fragments (13). The location of the other abundant component of the photosynthetic membrane, the cytochrome bc_1 complex, is not clear. Recent AFM and EM studies on *Rb. sphaeroides* membranes (8, 13) showed that the cytochrome bc_1 complex is not closely associated with the core dimer as suggested by Jungas *et al.* (7). The model presented here limits the possible location of the cytochrome bc_1 complex in the membrane because there appears to be no space left between the arrays of core and LH2 complexes as observed in the AFM images (13). Moreover, the dense packing of the membrane puts serious constraints on any diffusive mechanism for reduction of this complex by quinol as suggested in ref. 8. The asymmetry in the shape of these essentially spherical membranes could be a reflection of the partitioning of the membrane into specialized domains of not only LH2 but also of cytochrome bc_1 complexes.

Conclusions

We have probed native, intact, and untreated photosynthetic membranes of *Rb. sphaeroides* by using polarized-light spectroscopy on oriented membranes. The spectra demonstrate the special orientation of the RC within the LH1 ring and the existence of special domains enriched in LH2. Combining the results on an ensemble of intact membranes in this study with AFM images obtained on individual membrane patches (13), we derived a model for the organization of the most abundant complexes in a photosynthetic membrane. Some ordered arrangement of complexes has been observed, most commonly in photosynthetic membranes (8, 15, 19, 27). Such an organization is not essential for transporting excitation energy; but it could, rather, stem from the close packing of complexes within the membrane. For example: the hexagonal lattice of RC–LH1 core complexes as observed for the PufX- and LH2-lacking purple bacterium *Rhodopseudomonas viridis* (14) happens to be the most dense packing arrangement. Likely, the same holds for the *Rb. sphaeroides* membrane containing dimers of RC–LH1–PufX and LH2 complexes. The dense packing could reflect a necessity in very dim-light conditions when the absorption of every photon counts.

We thank Prof. Dr. Per Bullough and Dr. Bas Gobets for close reading of the manuscript. This work was supported by grants from The Netherlands Organization for Scientific Research through the Foundation of Earth and Life Sciences and the Biotechnology and Biological Sciences Research Council (U.K.).

1. Xiong, J., Fischer, W. M., Inoue, K., Nakahara, M. & Bauer, C. E. (2000) *Science* **289,** 1724–1730.
2. Des Marais, D. J. (2000) *Science* **289,** 1703–1705.
3. Overmann, J. (2001) *Microbiol. Today* **28,** 116–118.
4. Fleming, G. R. & van Grondelle, R. (1994) *Phys. Today* **47,** 48–55.
5. Lilburn, T. G., Haith, C. E., Prince, R. C. & Beatty, J. T. (1992) *Biochim. Biophys. Acta* **1100,** 160–170.
6. Barz, W. P., Verméglio, A., Francia, F., Venturoli, G., Melandri, B. A. & Oesterhelt, D. (1995) *Biochemistry* **34,** 15248–15258.
7. Jungas, C., Ranck, J.-L., Rigaud, J.-L., Joliot, P. & Verméglio, A. (1999) *EMBO J.* **18,** 534–542.
8. Siebert, C. A., Qian, P., Fotiadis, D., Engel, A., Hunter, C. N. & Bullough, P. A. (2004) *EMBO J.* **23,** 690–700.
9. McDermott, G., Prince, S. M., Freer, A. A., Hawthornthwaite-Lawless, A. M., Papiz, M. Z., Cogdell, R. J. & Isaacs, N. W. (1995) *Nature* **374,** 517–521.
10. Roszak, A. W., Howard, T. D., Southall, J., Gardiner, A. T., Law, C. J., Isaacs, N. W. & Cogdell R. J. (2003) *Science* **302,** 1969–1972.

11. Berry, E. A., Huang, L.-S., Saechao, L. K., Pon, N. G., Valkova-Valchanova, M. & Daldal, F. (2004) *Photosynth. Res.* **81,** 251–275.
12. Abrahams, J. P., Leslie, A. G. W., Lutter, R. & Walker, J. E. (1994) *Nature* **370,** 621–628.
13. Bahatyrova, S., Frese, R. N., Siebert, C. A., Olsen, J. D., van der Werf, K. O., van Grondelle, R., Niederman, R. A., Bullough, P. A., Otto, C. & Hunter, C. N. (2004) *Nature* **430,** 1058–1062.
14. Scheuring, S., Seguin, J., Marco, S., Lévy, D., Robert, B. & Rigaud J.-L. (2003) *Proc. Natl. Acad. Sci. USA* **100,** 1690–1693.
15. Scheuring S., Sturgis, J. N., Prima, V., Bernadac, A., Lévy, D. & Rigaud, J.-L. (2004) *Proc. Natl. Acad. Sci. USA* **101,** 11293–11297.
16. Kwa, S. L. S., Volker, S., Tilly, N. T., van Grondelle, R. & Dekker, J. P. (1994) *Photochem. Photobiol.* **59,** 219–228.
17. Abdourakhmanov, I. A., Ganago, A. O., Erokhin, Y. E., Solov'ev, A. A. & Chugunov, V. A. (1979) *Biochim. Biophys. Acta* **546,** 183–186.
18. Breton, J. (1985) *Biochim. Biophys. Acta* **810,** 235–245.
19. Frese, R. N., Olsen, J. D., Branvall, R., Westerhuis, W. H. J., Hunter, C. N. & van Grondelle, R. (2000) *Proc. Natl. Acad. Sci. USA* **97,** 5197–5202.
20. Niederman, R. A., Mallon, D. E. & Parks, L. C. (1979) *Biochim. Biophys. Acta* **555,** 210–220.
21. Hu, X., Ritz, T., Damjanovic, A., Autenrieth, F. & Schulten, K. (2002) *Q. Rev. Biophys.* **35,** 1–62.
22. Deisenhofer, J., Epp, O., Miki, K., Huber, R. & Michel, H. (1985) *Nature* **318,** 618–624.
23. Westerhuis, W. H. J., Vos, M., van Grondelle, R., Amesz, J. & Niederman, R. A. (1998) *Biochim. Biophys. Acta* **1366,** 317–329.
24. Papiz, M. Z., Prince, S. M., Hawthornthwaite-Lawless, A. M., McDermott, G., Freer, A. A., Isaacs, N. W. & Cogdell, R. J. (1996) *Trends Plant Sci.* **1,** 198–206.
25. Georgakopoulou, S., Frese, R. N., Johnson, E., Koolhaas, C., Cogdell, R., van Grondelle, R. & van der Zwan, G. (2002) *Biophys. J.* **82,** 2184–2197.
26. Sturgis, J. N. & Niederman, R. A. (1996) *Arch. Microbiol.* **165,** 235–242.
27. Boekema, E. J., van Breemen, J. F., van Roon, H. & Dekker, J. P. (2000) *J. Mol. Biol.* **301,** 1123–1133.